1 **Cloud Condensation Nuclei Activity of CaCO₃ Particles**

2 **with Oleic Acid and Malonic Acid Coatings**

3 **Mingjin Wang[1,2], Tong Zhu[1*], Defeng Zhao[2], Florian Rubach[2,3], Andreas**

4 **Wahner[2], Astrid Kiendler-Scharr[2], and Thomas F. Mentel[2*]**

5 [1]BIC-ESAT and SKL-ESPCl, College of Environmental Sciences and Engineering,

6 Peking University, Beijing 100871, China.

7 [2]Institut für Energie- and Klimaforschung (IEK-8), Forschungszentrum Jülich GmbH,

8 52425 Jülich, Germany.

9 [3]Klimageochemie, Max Planck Institut für Chemie, 55128 Mainz, Germany

11 [*] To whom correspondence should be addressed: tzhu@pku.edu.cn;

12 t.mentel@fz-juelich.de

14 **Abstract.**

15 Condensation of carboxylic acids on mineral particles will lead to coatings, and

16 impact on the particles' potential to act as cloud condensation nuclei (CCN). To

17 determine how the CCN activity of mineral particles is impacted by carboxylic acid

18 coatings, the CCN activity of CaCO₃ particles and CaCO₃ particles with oleic acid

19 and malonic acid coatings were compared in this study. The results revealed that small

20   amounts of oleic acid coating (volume fraction (vf) $\leq$ 4.1%) decreased the CCN

21   activity of $CaCO_3$ particles, while more oleic acid coating (vf $\geq$14.8%) increased the

22   CCN activity of $CaCO_3$ particles. This phenomenon has not been reported before. On

23   the other hand, malonic acid coating (vf = 0.4 - 42%) increased the CCN activity of

24    $CaCO_3$ particles regardless of the amount of the coating. The CCN activity of $CaCO_3$

25   particles with malonic acid coating increased with the amount of malonic acid coating.

26   Even smallest amounts of malonic acid coating (vf = 0.4%) significantly enhanced the

27   CCN activity of $CaCO_3$ particles from $\kappa = 0.0028 \pm 0.0001$ to $\kappa = 0.0123 \pm 0.0005$.

28   This supports that a small amount of water-soluble organic acid coating may

29   significantly enhance the CCN activity of mineral particles. The presence of about 50%

30   relative humidity during the coating process with malonic acid additionally increased

31   the CCN activity of the coated $CaCO_3$ particles, probably because more $CaCO_3$ reacts

32   with malonic acid at higher relative humidity.

1 Introduction

Atmospheric aerosols serve as cloud condensation nuclei and change the radiative properties (cloud albedo effect) and lifetime (cloud lifetime effect) of clouds, thus affecting the Earth's climate indirectly (Liu and Wang, 2010; Gantt et al., 2012; Penner et al., 2004; Haywood and Boucher, 2000). Mineral aerosol is one of the most abundant components of the atmospheric aerosol. It is estimated that 1500-2600 Tg of mineral aerosol particles with radii between 0.1 and 8 µm are emitted annually into the atmosphere on a global scale (Cakmur et al., 2006). Mineral aerosol particles are mainly composed of substances that are slightly soluble or insoluble in water. Cloud condensation nuclei (CCN) activity measurements show that the hygroscopicity parameter κ (Petters and Kreidenweis, 2007) varies between 0.001 and 0.08 for mineral aerosols, including $CaCO_3$ aerosol, clay aerosols and mineral dust aerosols generated in the laboratory or sampled from various locations worldwide (Garimella et al., 2014; Yamashita et al., 2011; Zhao et al., 2010; Koehler et al., 2009; Sullivan et al., 2010; Herich et al., 2009). The low κ indicates that the CCN activity of mineral aerosol is much lower than the CCN activity of water soluble salts like $(NH_4)_2SO_4$ (κ = 0.61) and NaCl (κ = 1.28), which are also common in atmospheric aerosols (Petters and Kreidenweis, 2007).

Mineral aerosol particles can be coated by organic gases during their residence and transport in the atmosphere. Many individual particle measurements have shown that mineral components and organic matter can coexist in the same individual aerosol particle in the real atmosphere (Falkovich et al., 2004; Falkovich et al., 2001; Russell

56   et al., 2002; Li and Shao, 2010). Carboxylic acids are abundant species among the

57   organic matter that coexists with mineral particles. Russell et al. (2002) found that

58   R(C=O)R, R(CH$_n$)R′ and R(C=O)OH are present in individual mineral (and sea salt)

59   aerosol particles, with enhanced concentration of R(C=O)OH. They also found that

60   Ca^{2+}, CO_3^{2-}, R(C=O)OH and R(C=O)R coexisted in some individual mineral aerosol

61   particles with a strong correlation between CO_3^{2-} and R(C=O)OH. These particles

62   could be formed by $CaCO_3$ particles (partly) coated with organic film. Falkovich et al.

63   (2004) also found that organic and inorganic components coexisted in individual

64   mineral aerosol particles with the organic component consisting of various short-chain

65   (C_1-C_{10}) mono- and dicarboxylic acids (MCA and DCA). The concentration of

66   short-chain carboxylic acids in mineral aerosol particles increased with the increase of

67   the ambient relative humidity. A possible explanation for such observations could be

68   that when more water is condensed onto mineral particles at higher ambient relative

69   humidity, the adsorbed carboxylic acids are ionized in the aqueous environment and

70   react with mineral particles forming organic acid salts. Of the major components of

71   mineral aerosol particles (clay, calcite ($CaCO_3$), quartz, mica, feldspar, etc.), only

72    $CaCO_3$ with alkaline character can react with carboxylic acids in this way. Thus

73    $CaCO_3$ may play a key role in the uptake of carboxylic acids by mineral aerosol

74   particles.

75   Carboxylic acid coatings on mineral aerosol particles change their chemical

76   composition and thus may have an impact on their CCN activity. Many previous

77   studies have investigated the CCN activity of pure mineral aerosol (Garimella et al.,

78   2014; Yamashita et al., 2011; Zhao et al., 2010; Koehler et al., 2009; Sullivan et al.,

79   2010; Herich et al., 2009) and pure carboxylic acid aerosol (Kumar et al., 2003; Hori

80   et al., 2003; Cruz and Pandis, 1997; Hartz et al., 2006), but only a few studies have

81   investigated the CCN activity of mineral aerosol particles with carboxylic acid

82   coatings (Tang et al., 2015; Hatch et al., 2008; Gierlus et al., 2012).

83   In this study we used malonic acid and oleic acid as coating materials and $CaCO_3$

84   particles as cores, and investigated the CCN activity of the coated $CaCO_3$ particles.

85   Herein we varied the coating thickness and the relative humidity during the coating

86   process. Malonic acid is a representative of the class of dicarboxylic acids and oleic

87   acid is an example of surfactant like compounds. Dicarboxylic acids are ubiquitous in

88   the atmosphere (Kawamura et al., 1996; Kawamura and Ikushima, 1993; Ho et al.,

89   2007; Mkoma and Kawamura, 2013; Kawamura and Bikkina, 2016) and formed by

90   photochemical reactions and ozonolysis (Chebbi and Carlier 1996; Kawamura and

91   Bikkina, 2016; Kawamura et al., 1996; Khare et al. 1999; Mellouki et al., 2015). It has

92   been reported that dicarboxylic acids (C_2-C_{10}) account for 0.06-1.1% of the total

93   aerosol mass, with higher values in the summer, and 1.8% of the total aerosol carbon

94   (TC) in urban aerosol, in which oxalic acid, malonic acid, and succinic acid are the

95   most abundant species (Kawamura et al., 1996; Kawamura and Ikushima, 1993; Ho et

96   al., 2007; Mkoma and Kawamura, 2013). Oleic acid, which is emitted into the

97   atmosphere by the cooking of meat, wood burning, and automobile source (Schauer et

98   al., 1999; Rogge et al., 1998; Rogge et al., 1993), is present in atmospheric aerosols of

99   urban, rural, and forest areas (Cheng et al., 2004; Ho et al., 2010). The water

100   solubility of the two organic acids is complementary; it is high for malonic acid while

101   it is very low for oleic acid. Coatings of malonic acid and oleic acid could thus have

102   different effects on CCN activity of mineral particles.

103

104

2 Experimental

106 As general procedure, $CaCO_3$ aerosol was generated according to Zhao et al. (2010),

107 and then poly- or monodisperse $CaCO_3$ aerosol particles were coated by malonic or

108 oleic acid in a coating device. A flow tube was optionally applied to extend the

109 residence time. The particle size, chemical composition, and CCN activity of the

110 $CaCO_3$ particles were measured before and after coating. Figure 1 shows the

111 schematic of the experimental set up.

2.1 Generation of CaCO₃ aerosol

113 $CaCO_3$ aerosol was generated by spraying a saturated $Ca(HCO_3)_2$ solution. A sample

114 of $CaCO_3$ powder (2 g, pro analysis, ≥99%, Merck, Darmstadt, Germany) was

115 suspended in 1-L Milli-Q water (18.2 MΩcm, TOC <5 ppb). Then about 1.5 L min^{-1}

116 CO_2 (purity ≥99.995%, Praxair Industriegase GmbH & Co. KG, Magdeburg,

117 Germany) was bubbled into the suspension at room temperature for 3 h, while the

118 suspension was stirred using a magnetic stirrer. During bubbling, CO_2 reacted with

119 $CaCO_3$ to produce $Ca(HCO_3)_2$. After bubbling, the suspension was allowed to settle

120 for 10 min, the supernatant clear $Ca(HCO_3)_2$ solution was decanted and used for

121 spraying by a constant output atomizer (Model 3076, TSI, Shoreview, MN, USA)

122 using 1.75 L min^{-1} high-purity N_2 (Linde LiPur 6.0, purity 99.9999%, Linde AG,

123 Munich, Germany).

124

125   The major portion (0.9 L min^{-1}) of the aerosol flow generated by spraying was dried

126   in a diffusion drier filled with silica gel. The relative humidity was below 10% after

127   drying. The remainder of the aerosol flow was drawn off by a pump and discarded.

128   The dry aerosol was passed through a tube furnace (Model RS 120/1000/12,

129   Nabertherm GmbH, Lilienthal, Germany) set at 300 ºC. The residence time of the

130   aerosol in the furnace was 5.2 s. Zhao et al. (2010) described this method for

131   generating $CaCO_3$ aerosol in detail. At room temperature dry $Ca(HCO_3)_2$ is

132   thermodynamically unstable and decays into $CaCO_3$, CO_2, and H_2O (Keiser and

133   Leavitt, 1908). With this method the aerosol still contained some $Ca(HCO_3)_2$ after

134   drying, but after heating at 300 ºC it was completely converted into $CaCO_3$ (Zhao et

135   al., 2010). The $CaCO_3$ aerosol generated was either first size selected by a Differential

136   Mobility Analyzer (DMA, TSI 3081) with a neutralizer on the inlet or entered the

137   coating device directly as poly-disperse aerosol.

138   Figure 2 (upper panel) shows the total number concentration and mean size of the

139   bare $CaCO_3$ aerosol particles generated at different spraying time, which were

140   measured with the SMPS described below. The diameter size stabilized after about 50

141   min in the range 49.8-55.5 nm. Over the 232 min spraying time, the total number

142   concentration varied in the range 1.8×10^6–4.5×10^6 cm^{-3}. The total number

143   concentration decreased by about 1/3 in the initial 70 min. The decrease became

144   slower after 70 min and the total number concentration tended to stabilize after 155

145   min. After 70 min the total number concentration varied in a smaller range of

146   1.8×10^6–2.9×10^6 cm^{-3}, therefore, the measurements in this study typically started after

147   70 min spraying. The typical size distribution of the CaCO₃ aerosol particles after 70

148   min spraying is shown in Fig. 2 (lower panel). The CaCO₃ particles showed a single

149   mode distribution with a mode diameter at 32.2 nm. The number concentration was

150   more than 100 cm^{-3} for particles between 9.82 and 346 nm.

2.2 Organic acid coating

152   The coating device (Fig. 1, right hand side) used in this study was designed by Roselli

153   (2006), and showed good reproducibility, controllability, and stability. The glass

154   apparatus consisted of a small storage bulb (100 ml) holding the organic coating

155   substances which was directly connected to a mixing cell (about 35 ml). The storage

156   bulb and mixing cell were fully immersed in a flow-through water heater connected to

157   a thermostatic bath (F25, Julabo GmbH, Seelbach, Germany). The temperature range

158   of the thermostatic bath used in this study was 30-80 ºC. An extra N_2 stream could be

159   passed through the storage bulb in order to enhance the organic vapors flowing into

160   the mixing cell. The outflow of the coating device was connected to a Liebig type

161   water cooler. The water cooler was controlled by another thermostatic bath (F25,

162   Julabo GmbH, Seelbach, Germany) operated at 25 ºC throughout all of the

163   experiments.

164   The bottom of the storage bulb was filled with either 5.0 g malonic acid powder

165   (assay ≥98%(T), Fluka Chemika, Sigma-Aldrich, St Louis, MO, USA) or 10.0 ml

166   oleic acid (chemical purity (GC) 99.5%, Alfa Aesar, Ward Hill, MA, USA). A flow of

167   0.9 L min^{-1} high purity N_2 was used to carry the organic acid vapor up into the mixing

168   cell. The flow of 0.9 L min^{-1} CaCO₃ aerosol was passed through the mixing cell and

169   mixed with the 0.9 L min^{-1} N_2 flow carrying the organic acid vapor. The mixed flow

170   then entered the water cooler. The organic acid vapor was condensed on CaCO₃

171   aerosol particles in both the mixing cell and the water cooler. Three identical coating

172   devices, with the same heating and cooling thermostatic bath, were used: one for

173   malonic acid coating, one for oleic acid coating, and a blank one without organic acid

174   for assessing the impact caused by heating the CaCO₃ aerosol in the coating device

175   without organic acid (Roselli, 2006).

176   The aerosol could enter the measuring instruments directly, or after passing through a

177   flow tube to increase its residence time. The flow tube was made of a straight circular

178   glass tube with a 2.5 cm internal diameter. The aerosol flow in the flow tube was

179   laminar flow. The residence time of the aerosol in the flow tube was 23.7 s.

180   The relative humidity of the aerosol at the outlet of the coating device at 80 ℃ was

181   below 5%. To investigate the impact of relative humidity on the coating process and

182   CCN activity, organic coating at a higher relative humidity was also performed. For

183   that a bubbling device filled with Milli-Q water placed in the N_2 stream before it

184   entered the storage bulb. The relative humidity of the aerosol at the outlet of the

185   coating device at 80 ℃ was ~47% when humidification was applied.

2.3 Size and chemical composition measurements

187   The number size distribution of the aerosol particles was measured using a Scanning

188   Mobility Particle Sizer (SMPS, TSI 3080 Electrostatic Classifier with TSI 3081 DMA,

189   TSI 3786 UWCPC). The sample flow was set to 0.6 L min⁻¹ and the sheath flow was

190   set to 6.0 L min⁻¹. The size range measured was 9.82-414.2 nm and the time

191   resolution was 3 min for a complete scan.

192

193   The chemical composition and the vacuum aerodynamic diameter of the aerosol

194   particles were measured using a High-Resolution Time-of-Flight Aerosol Mass

195   Spectrometer (HR-ToF-AMS, Aerodyne Research Inc., Billerica, MA, USA (DeCarlo

196   et al., 2006)). The aerosol particles were vaporized at 600 ºC and ionized by 70 eV

197   electron impact ionization, i.e. we focused on the measurements of the organic

198   coatings and sacrificed a direct $CaCO_3$ determination by AMS (compare Zhao et al.

199   2010). The AMS was routinely operated in V-mode in two alternating modes: 1 min

200   MS mode to measure the chemical composition and 2 min PToF mode. Only MS

201   mode data were analyzed. AMS measurements and SMPS measurements were

202   synchronous and both were repeated at least four times for each sample. Size

203   information for bare $CaCO_3$ was taken from SMPS data in the blank coating device.

204   We used specific marker m/z to derive the amount of organic coating. For pure oleic

205   acid the signal at $m/z41$ ($C_3H_5^+$) was reported to be the strongest signal in the mass

206   spectrum measured by Q-AMS at EI energy of 70 eV and vaporizer temperature of

207   600 ºC (Sage et al., 2009). The signal at $m/z41$ was also strongest for oleic acid

208   coatings in our HR mass spectra. In order to get a high signal to noise ratio we

209   analyzed the signal at $m/z41$ in the MS mode of the AMS measurement as a marker

210   for oleic acid in the coated $CaCO_3$ particles. There was no significant signal at $m/z41$

211   for the uncoated $CaCO_3$ particles. The average background signal at $m/z41$ per single

212   aerosol particle corresponded to $2.4\pm0.79\cdot10^{-12}$ µg for bare $CaCO_3$. The average value

213   presented the baseline of the mass spectra and the standard deviation was derived

214   from the noise of the mass spectra at $m/z41$. Similarly, the signal at $m/z42$ ($C_2H_2O^+$)

215   was one of the strongest signals in the mass spectrum of pure malonic particles

216   measured by Q-AMS with EI energy of 70 eV and vaporizer temperature of 600 ºC

217   (Takegawa et al., 2007). That signal was also observed for malonic acid coatings in

218   our HR mass spectra and used as marker for malonic acid coatings. The average

219   background signal per aerosol particle at $m/z42$ for bare $CaCO_3$ particles was

220    $1.4\pm0.42\cdot10^{-12}\mu g$. The average value represented the baseline of the mass spectra at

221    $m/z42$ and the standard deviation was derived from the noise in the mass spectra.

222   The coating amount for both organic compounds was derived as follows. The

223   observed signal at the respective marker m/z was corrected for the background signal

224   from bare $CaCO_3$ and then scaled to the volume increase (per particle) calculated

225   from the shift of the mode diameter for the largest coating amount achieved at 80 ºC

226   coating temperature. This assumed spherical core shell morphology, based on Zhao et

227   al. (2011) where we showed that the $CaCO_3$ particles generated by our spray drying

228   method are spherical. The baseline corrected marker signals at $m/z41$ or $m/z42$ per

229   particle were in direct proportion with the oleic acid mass per particle and malonic

230   acid mass per particle, respectively. Coating mass per particle was in direct proportion

231   with the coating volume per particle. So V_{OA} for coating temperatures of 30-70 ºC

232   could be calculated from the largest V_{OA} and the marker signals per particle at $m/z41$

233   and $m/z42$.

234   Assumption of spherical geometry and sub-scale mode shift within the bin width of

235   the SMPS introduces uncertainties in the determination of the amount of coatings. We

236   therefore prefer to show the experimental data as a function of the controlling

237   parameter, the coating temperature. In the discussion we also use the coating mass per

238   particle to give an easier to imagine rationale to the finding and classification.

239

2.4 CCN activity measurement

240

241 The aerosol was dried to RH <3% by another diffusion drier before the CCN activity

242 was measured. To determine the CCN activity of the aerosol, the number

243 concentration of the cloud condensation nuclei (CCN) of the aerosol was measured

244 with a continuous flow CCN counter (CCNC, DMT-100, Droplet Measurement

245 Technologies, Boulder, CO, USA). The total number concentration (CN) of the

246 aerosol particles was synchronously measured using an ultrafine water-based

247 condensation particle counter (UWCPC, TSI 3786, cf. Zhao et al., 2010). The ratio of

248 CCN to CN (CCN/CN) is called the activated fraction (a_f). In cases where

249 poly-disperse aerosol was coated, the coated aerosol particles were size selected by

250 scanning a DMA between 10.6 and 478.3 nm , and the CCN and CN concentrations

251 were determined for each size bin while the super-saturation (SS) kept constant

252 (known as 'Scanning Mobility CCN Analysis (SMCA)', Moore et al., 2010). The

253 activated fraction was calculated after the CCN and CN concentrations were corrected

254 for the multiple charged particles.

255 The activated fraction as a function of the particle size was fitted with a cumulative

256 Gaussian distribution function (Rose et al., 2008). The turning point of the function is

257 the critical dry diameter (D_{crit} or D_{50}) at the set SS. The activation efficiency (i.e., the

258 activated fraction when aerosol particles are completely activated) was 83% for the

259 CCN instrument, determined using 150 nm $(NH_4)_2SO_4$ particles at SS=0.85%.

260 Besides $CaCO_3$ and coated $CaCO_3$ particles, the CCN activity of malonic acid

261 particles, oleic acid particles, and mixed particles of $CaCO_3$ and malonic acid was

262 also measured. The oleic acid particles were generated by heating 10.0 ml oleic acid

263 to 97 ºC in the storage bulb and then cooling the vapor to 2 ºC in the water cooler in a

264   clean coating device. 1.75 L min^{-1} high-purity N$_2$ was used as carrying gas and went

265   into the storage bulb through'1 N$_2$ in' entrance in Fig. 1; the'3 Aerosol in' entrance in

266   Fig. 1 was closed. This way, pure oleic acid particles with diameters up to 333 nm

267   were generated. Mixed CaCO$_3$/malonic acid particles were generated by spraying the

268   supernatant clear solutions which were prepared by settling suspensions containing

269   CaCO$_3$ and malonic acid in molar ratios of about 1:1 and 3:1. The suspensions were

270   prepared with 0.020 g malonic acid and 0.021 g CaCO$_3$ and 0.025 g malonic acid and

271   0.076 g CaCO$_3$ in 1000 ml Milli-Q water, respectively. The suspensions were allowed

272   to stand for 24h.

273   For aerosols where monodisperse aerosol particles with a dry diameter D$_p$ were coated,

274   the CCN concentration was measured at different SS and the CN concentration was

275   measured synchronously. Similarly, the activated fraction as a function of SS was

276   fitted with a cumulative Gaussian distribution function. The turning point of the

277   function is the critical super-saturation (SS$_{crit}$) and the corresponding to the dry

278   diameter D$_p$ is also called the critical diameter, D$_{crit}$. The hygroscopicity parameter κ

279   (Petters and Kreidenweis, 2007) was then calculated from the D$_p$(D$_{crit}$)-SS$_{crit}$ or

280   SS(SS$_{crit}$)-D$_{crit}$ data set. The SS settings of the CCN counter were calibrated weekly

281   using (NH$_4$)$_2$SO$_4$ aerosol based on the theoretic values in the literature (summarized

282   by Rose et al., 2008).

283

3 Results and discussion

3.1 CCN activity of CaCO₃ aerosol

Before the coating experiments we determined the CCN activity of the bare $CaCO_3$

aerosol particles generated. It was measured by the scanning method (SMCA) using

poly-disperse $CaCO_3$ aerosol particles. The value of the hygroscopicity parameter κ of

the $CaCO_3$ aerosol was 0.0028 ± 0.0001 derived by the least-square-fitting of D_{crit} as a

function of SS (SS_{crit}). This κ value is quite small, indicating that the CCN activity of

the $CaCO_3$ aerosol is low. In previous studies κ for the $CaCO_3$ aerosol was found in

the range 0.0011 ± 0.0004 to 0.0070 ± 0.0017 (Zhao et al., 2010; Sullivan et al., 2009;

Gierlus et al., 2012) and our κ value is somewhat higher but still in this range. The

CCN activity for $CaCO_3$ aerosol passed through the blank coating device exposed to

temperatures of 60 ºC and 80 ºC was measured using the same method. The κ value

remained 0.0028 ± 0.0001 at 60 ºC and increased to 0.0036 ± 0.0001 at 80 ºC. The

CCN activity of the $CaCO_3$ aerosol after heating was the same or slightly higher than

that of the $CaCO_3$ aerosol without heating. The increased κ value of 0.0008 at 80 ºC

was lower than the differences of reported κ values for $CaCO_3$ aerosol in various

studies, and much lower than the changes of κ values measured in this study when the

$CaCO_3$ aerosol particles were coated by malonic or oleic acid. So the effect of heating

the $CaCO_3$ aerosol during the coating process on the CCN activity of the $CaCO_3$

aerosol was neglected. The D_{crit} at different super-saturations (SS_{crit}) for the $CaCO_3$

304   aerosol and for the CaCO₃ aerosol passed through a blank coating device at heating

305   temperatures of 60 ºC and 80 ºC are shown in Fig. 5 (red, yellow and green circles).

3.2 CCN activity of CaCO₃ particles with oleic acid coating

306

307   For the coating with oleic acid, we selected monodisperse CaCO₃ aerosol particles of

308   101.8 nm diameter using the DMA, and measured the size and chemical composition

309   of the particles before (uncoated) and after (coated) coating with oleic acid. The

310   results are listed in the upper part of Table 1. In order to achieve coatings with various

311   amounts of oleic acids the CaCO₃ particles were passed through the coating device

312   containing 10.0 ml oleic acid held at different temperatures in a range of 30-80 ºC.

313   The uncoated CaCO₃ particles passed through the blank (empty) coating device at the

314   same respective temperature.

315   The mode diameters of number size distribution for the uncoated CaCO₃ particles at

316   30-80 ºC remained 101.8 nm, identical to that selected by the DMA. The mode

317   diameters of the CaCO₃ particles after coating with oleic acid in the range of 30-50 ºC

318   stayed also in the pre-selected size bin at 101.8 nm, which means that the layers were

319   too thin to effectively grow the particles to the next size bin. However, the mode

320   diameters increased distinctively with the increase of the coating temperature in the

321   temperature range of 60-80 ºC (Fig. 3, upper panel). This shows that temperatures of

322   60-80 ºC were needed to sufficiently increase the vapor pressure of the oleic acid to

323   get significant amounts of oleic acid coating onto the CaCO₃ particles. Once the

324   coating temperature exceeded a certain value the amount of the coating increases with

325   the increase of the coating temperature.

326   The values of m/z41 [µg] per particle originating from the oleic acid coating for the

327   coated $CaCO_3$ particles at 30-80 ºC were at all temperatures significantly larger than

328   for the bare $CaCO_3$ particles, and increased with the increasing coating temperature

329   ($3.3 \cdot 10^{-12}$ - $350 \cdot 10^{-12}$ µg per particle, compare Table 1 and Fig. 3, bottom panel, red

330   circles). The AMS detected increase at $m/z41$ showed that the $CaCO_3$ particles already

331   contained small amounts of oleic acid after coating with oleic acid at temperatures

332   below 60 ºC although the mode diameter did not shift.

333   The organic volume fraction (vf) in the aerosol particles, V_{OA}/V_{par} [%], was calculated.

334   Herein $V_{par} = (V_{OA} + V_{CaCO3})$, V_{OA} is the oleic acid volume derived by AMS and

335   V_{CaCO3} the volume of the bare $CaCO_3$ before coating (101.8 nm). V_{OA}/V_{par} for the

336   uncoated $CaCO_3$ particles is by definition zero. The vf for the coated $CaCO_3$ particles

337   at 30-80 ºC increased with the increase in the coating temperature from 0.7% at 30 ºC

338   to 41.8% at 80 ºC (Fig. 3, bottom panel, red crosses and Table 1). The AMS data thus

339   show that at 30-80 ºC the $CaCO_3$ particles were indeed coated with a significant

340   amount of oleic acid and the amount of oleic acid coating increased with the increase

341   in the coating temperature. The experiments were repeated at least four times. The

342   mode diameters were identical each time and the according standard deviations for the

343   oleic acid mass per particle in Table 1 indicate that the repeatability of the

344   experiments was good and the performance of the coating device was stable.

345   The activated fractions at different SS for monodisperse CaCO$_3$ particles selected at

346   101.8 nm before and after oleic acid coating at 30-80 ℃ are shown in Fig. 4. The top

347   panel in Fig. 4 shows the results at 30-60 ℃ with small amounts of coating material

348   deposited on the CaCO$_3$ particles. At the lowest SS of 0.17% and 0.35%, the activated

349   fractions were very low and independent of the presence of the coating material

350   within the errors. When the SS increased to 0.52%, 0.70%, and 0.87%, the activated

351   fractions for the coated CaCO$_3$ particles were lower than those for the uncoated

352   particles. Interestingly the activated fractions for the coated CaCO$_3$ particles

353   decreased with the increase in the coating temperature at 30-50 ℃, thus with the

354   increase in the coating material (vf 0.7-2.5%). The activated fractions for the CaCO$_3$

355   particles with different amounts of coating spread with larger SS applied. However

356   this trend reversed at the coating temperature of 60 ℃ and the oleic acid vf of 4.1%,

357   and the activated fractions at 60 ℃ became higher than those at 50 ℃ at the three

358   largest SS. Considering the invariant mode diameter at 30-50 ℃, the increased mode

359   diameter at 60 ℃, and the reduced activated fraction simultaneously, we found that

360   the CCN activity of the coated CaCO$_3$ particles at 30-60 ℃ was lower than that of the

361   uncoated CaCO$_3$ particles. The CCN activity of the coated CaCO$_3$ particles at 30-50

362   ℃ decreased with the increase in the coating temperature, i.e. the CCN activity

363   became lower when more coating material deposited on the CaCO$_3$ particles.

364   The activated fractions of CaCO$_3$ particles after coating with oleic acid at 70 and 80

365   ℃ (vf 14.8% and 41.8%, respectively) were considerably higher than that before

366   coating, as shown in Fig. 4 (bottom panel). The increased activated fractions resulted

367 from both the increase in particle size (Fig. 3) and the change in chemical

368 composition (hygroscopicity) of particles. At 70 and 80 ºC, the activated fractions of

369 the CaCO$_3$ particles after coating increased with the increase of SS and reached a

370 plateau at high SS. The plateau indicated that the aerosol particles were completely

371 activated. Because the activation efficiency is 83%, the activated fractions appear at

372 values less than 100% at the points of full activation. SS$_{crit}$ was determined by

373 Gaussian fitting of the activated fraction as a function of SS. The particle dry diameter

374 D$_p$ which is D$_{crit}$ in this cases was determined with SMPS and is given as the mode

375 diameter in Table 1. The hygoscopicity parameter κ was determined from D$_p$ (D$_{crit}$)

376 and the corresponding SS$_{crit}$. The κ values of the CaCO$_3$ particles coated with vf of

377 oleic acid of 14.8 % (70 ºC) and 41.8% (80 ºC) were 0.0237 ± 0.0006 and 0.0673 ±

378 0.0016, respectively. The respective κ values for the CaCO$_3$ particles with a diameter

379 of 101.8 nm without coating and after coating with oleic acid at 30-60 ºC (oleic acid

380 vf ≤4.1%) could not be determined by this method because these particles could not

381 be fully activated at the highest SS reachable by the CCN counter. Therefore we can

382 only give as upper limit κ = 0.0028 ± 0.0001 for the uncoated CaCO$_3$ particles

383 determined by scanning the size of the poly-disperse CaCO$_3$ aerosol particles as

384 described above (see Fig. 5). So we conclude that for vf of oleic acid of 0.7-2.5% the

385 CCN activity of CaCO$_3$ particles after coating is lower than that of uncoated CaCO$_3$

386 particles and decreases with the fraction of oleic acid. The trend turns at a vf of about

387 4.1%. CCN activity was higher than that of the bare CaCO$_3$ particles at vf of oleic

388 acid of 14.8% and 41.8% with CCN activity κ = 0.0237 ± 0.0006 and κ = 0.0673 ±

389   0.0016), respectively. In addition, the enhanced and reduced CCN activity of $CaCO_3$

390   particles coated with oleic acid at 80 ºC and 60 ºC, respectively, was also evident

391   from the CCN activity measurement using *poly-disperse* aerosols (Fig. 5).

392   The results presented above show that the CCN activity of the $CaCO_3$ particles

393   decreased after coating with small amounts of oleic acid at 30-60 ºC (oleic acid vf $\leq$

394   4.1%), but increased after coating with larger amounts of oleic acid at 70 and 80 ºC

395   (oleic acid vf of 14.8 and 41.8%). The coating temperature of 60 ºC, at which the

396   oleic acid vf of the coated $CaCO_3$ particles was 4.1%, seemed to be near the turning

397   point but we could not determine it precisely. The activated fractions indeed began to

398   increase at 60 ºC, but the mode diameter also increased at 60 ºC. Therefore we cannot

399   differentiate if the increase in the activated fractions is due to higher CCN activity or

400   the increase in the particle size. In any case our findings indicate that different

401   amounts of oleic acid coating have different impacts on the CCN activity of $CaCO_3$

402   particles.

403   A possible explanation for our observation can be based on the amphiphilic character

404   of oleic acid, namely that one end of the oleic acid molecule is hydrophobic (the

405   hydrocarbon chain), while the other is hydrophilic (the carboxyl group). When $CaCO_3$

406   particles are coated with only a small amount of oleic acid, the hydrophilic end of the

407   oleic acid molecule tends to combine with the hydrophilic sites on the surface of

408   $CaCO_3$. As a result, the hydrophobic end of the molecule is exposed on the particle

409   surface, hence increases the hydrophobicity of the particle surface. This can hinder the

410   uptake of water. When $CaCO_3$ particles are coated with more oleic acid, a kind of

411   bilayer may be formed with a portion of the hydrophilic ends of oleic acid molecules

412   pointing outward be exposed on the particle surface. The particle surface then

413   becomes more hydrophilic. This suggestion is supported by very low CCN activity of

414   pure oleic acid if one assumes that in pure oleic acid particles the hydrophobic tale is

415   exposed at the outside. Kumar et al. (2003) found that oleic acid particles up to 140

416   nm do not activate at 0.6% SS, and Broekhuizen et al. (2004) found that particles up

417   to 300 nm do not activate at 1% SS. Our CCN activity measurements showed that

418   oleic acid particles up to 333 nm do not activate at 0.87% SS. These data set the upper

419   limits of κ of pure oleic acid to 0.012 and $<10^{-6}$, respectively, comparable to our

420   thinly coated particles and more than a factor of two smaller than for our thickly

421   coated particles. Another factor that can contribute to the enhanced CCN activity at

422   high oleic acid fractions is the decrease of surface tension. Surface of tension of pure

423   oleic acid is only ~30 mN m^{-1} (Chumpitaz et al., 1999).

424   Garland et al. (2008) studied sub-monolayer deposition of oleic acid on both

425   hydrophobic and hydrophilic surfaces. Their results suggested that individual oleic

426   acid molecules were oriented vertically on the surfaces and the hydrocarbon chain of

427   the oleic acid molecule was facing away from the surface. According to the

428   measurements and calculations of the length of oleic acid molecule, the thickness of

429   oleic acid sub-monolayer on solid surface, and the thickness of deuterated oleic acid

430   monolayer at the air-water interface (Garland et al., 2008; King et at., 2009; Iwahashi

431   et al., 2000), we determined 2.3 nm as the likely thickness of oleic acid monolayer on

432   CaCO₃ particles. The mode diameters of the coated CaCO₃ particles at 30-60 ℃ show

433   that the oleic acid coating layers must have been sub-monolayers. As a consequence

434   small but increasing amounts of oleic acid coatings passivated the CaCO₃ surface by

435   pointing outward the hydrophobic tails. The mode diameters of the coated CaCO₃

436   particles at 70-80 ℃ show that the oleic acid coating layers were thicker than

437   monolayer. Although we cannot proof the structures of the oleic acid coating layers in

438   this case, we suppose that hydrophilic ends of a certain fraction of the oleic acid

439   molecules could be exposed on the particle surface.

440   The phenomenon described above is reported for the first time in the studies on the

441   CCN activity of multicomponent aerosols. This phenomenon also shows a limitation

442   of the otherwise very useful mixing rule (Petters and Kreidenweis, 2007) for

443   multicomponent aerosols with specific morphologies.

444   In Fig. 5 we additionally show the influence of the relative humidity on CCN activity

445   of CaCO₃ particles coated with oleic acid for the highest coating temperature (80 °C)

446   and thus largest oleic acid amount. Herein we determined D_{crit} at different

447   super-saturations (SS_{crit}) for *poly-disperse* CaCO₃ aerosol particles (by SMCA). The

448   experiments at a coating temperature of 80 °C at RH ≤5% and at RH 47% were

449   performed. The presence of water in the coating process increases κ somewhat and

450   enhances the CCN activity. This is of importance since often RH will larger than 5%

451   if coating appears in the atmosphere. This will be discussed further in context of

452   malonic acid coatings at RH 47%.

3.3 CCN activity of CaCO$_3$ particles with malonic acid coating

453

454 For the study with malonic acid coatings, the CaCO$_3$ particles were also size selected

455 with a diameter of 101.8 nm. The size and chemical composition of CaCO$_3$ aerosol

456 particles are listed in Table 1 before and after coating with malonic acid at

457 temperatures in a range of 30-80 ℃. The mode diameter did not shift after coating in a

458 temperature range of 30-60 ℃, but it increased for coatings at 70 and 80 ℃ with

459 increasing coating temperature.

460 Values of m/z42 per particle originating from malonic acid coating were significantly

461 larger for CaCO$_3$ particles after coating at 30-80 ℃ and increased with the increase of

462 the coating temperature (Table 1). The organic volume fraction vf of malonic acid

463 ($V_{MA}/(V_{MA}+V_{CaCO3})$[%]) was calculated as in the case of the oleic acid. The malonic

464 acid vf of the CaCO$_3$ particles after coating increased with the increase of the coating

465 temperature. At 30-60 ℃, the organic vf increased but this is not reflected in the mode

466 diameters. At these coating temperatures the layer of malonic acid coating was too

467 thin to effectively grow the particles to the next size bin. The AMS results however

468 showed that in the whole range of coating temperatures of 30-80 ℃ the CaCO$_3$

469 particles were coated by a significant and increasing amount of malonic acid. As in

470 the case of oleic acid the malonic acid experiments were repeated at least four times

471 and the repeatability and stability were good (see standard deviations in Table 1).

472 The activated fractions at different SS for 101.8 nm CaCO$_3$ particles before and after

473 coating with malonic acid at 30-80 ℃ are shown in Fig. 6. SS$_{crit}$ was determined from

474   Gaussian fitting of the data and the κ value was calculated from the D_p (D_{crit}) and the

475   corresponding SS_{crit}. The results are listed in Table 1. The κ values of the $CaCO_3$

476   particles after coating with malonic acid at 30-80 ℃ were higher than the κ value of

477   the uncoated $CaCO_3$ particles ($\kappa = 0.0028 \pm 0.0001$), and increased with the

478   increasing coating temperature and thus increasing malonic acid vf of 0.5-42%. The

479   CCN activity of the $CaCO_3$ particles increased monotonically after coating with

480   increasing malonic acid vf. This result differs from that of oleic acid which is not

481   surprising since malonic acid is easily soluble in water.

482   The κ value for the $CaCO_3$ particles after coating with malonic acid at 30 ℃ was

483   0.0123 ± 0.0005, which was considerably larger than the κ value for the uncoated

484      $CaCO_3$ particles ($\kappa = 0.0028 \pm 0.0001$). The $CaCO_3$ particles after coating with

485   malonic acid at 30 ℃ contained only 0.4% (vf) organic matter. This suggests that

486   already a small amount of malonic acid can significantly enhance the CCN activity of

487      $CaCO_3$ particles. Such phenomenon, that traces of water soluble substances can

488   strongly affect droplet activation has been reported before (Bilde and Svenningsson,

489   2004).

490   The D_{crit} at different super-saturations (SS_{crit}) for *poly-disperse* $CaCO_3$ aerosol

491   particles before and after coating with malonic acid are shown in Fig. 7. Our

492   observation of $\kappa = 0.25 \pm 0.04$ for pure malonic is consistent with the κ derived from

493   the data of Kumar et al. (2003) ($\kappa = 0.20\text{-}0.25$) and Prenni et al. (2001) ($\kappa = 0.24$), but

494   significantly lower than the κ derived from the data of Giebl et al. (2002) ($\kappa =$

495   0.41-1.04). The CCN activity of the $CaCO_3$ particles after coating at 60 and 80 ºC was

496   higher than that of the uncoated $CaCO_3$ particles, and the CCN activity at 80 ºC

497   (yellow triangles) was higher than that at 60 ºC (green triangles). The behavior of

498   poly-disperse coated aerosol was similar to the result obtained from the monodisperse

499    $CaCO_3$ aerosol particles.

500   In Fig. 7 we added results for coating at RH = 47% and aerosols generated by

501   spraying mixtures of malonic acid and $CaCO_3$. At the coating temperature of 60 ºC,

502   when the RH increased from ≤5% to 47%, the CCN activity of the coated $CaCO_3$

503   particles increased substantially (compare ≤5% (blue triangles) and 47% (lilac

504   triangles) in Fig. 7). The effect is more distinct than for the oleic acid coating shown

505   in Fig. 5, and κ increases by about an order of magnitude. At a higher RH, the

506   reaction between $CaCO_3$ and malonic acid is obviously more efficient and forms more

507   calcium malonate and this may be the reason for the higher CCN activity at the higher

508   RH. The hypothesis of efficient malonate formation is supported by the CCN activity

509   of "calcium malonate" aerosols, generated by spraying solutions containing $CaCO_3$

510   and malonic acid with molar ratios of about 1:1 and 3:1. Here the CCN activity is

511   similar to that arising in the coating process at 47% RH. The change of the

512   Ca/malonate ratio from 3:1 to 1:1 had no large effects. But taking the data of pure

513   malonic acid particles also into account there is a trend to lower κ with increasing Ca

514   in the initial solution.

515

516   The increasing of residence time (by 23.7 s) had no significant impact on CCN

517   activity for both oleic acid coating and malonic acid coating at both dry and 47% RH

518   conditions, probably because the coating process was already completed in the

519   coating device and no further reactions occurred in the flow tube.

520   Our findings may be important for aging processes of mineral particles in the

521   atmosphere. The dependence of CCN activity of the coated particles on RH during the

522   coating process will help to enhance the increase of the CCN activity by the coating

523   process as water will be abundant in many instances. The effect probably will be

524   relatively small for oleic acid and similar organics, which are hardly water soluble,

525   but strong for malonic acid and similar organic acids, which are highly water soluble.

526   **4 Conclusions**

527   The CCN activity of $CaCO_3$ particles with oleic acid and malonic acid coatings was

528   investigated in this study. The results show that oleic acid coating and malonic acid

529   coating have different impacts on the CCN activity of $CaCO_3$ particles. This can be

530   attributed to the amphiphilic property of oleic acid in contrast to the high water

531   solubility of malonic acid. Small amounts of oleic acid coating (vf ≤ 4.1%) decreased

532   the CCN activity of the $CaCO_3$ particles, while more oleic acid coating (vf ≥14.8%)

533   increased it. This phenomenon was reported here for the first time, and attributed to

534   stepwise passivating the active sites of $CaCO_3$ by oleic acid. Once all active sites are

535   occupied we suggest the formation of a bi-layer (micelle like) with the carboxylic

536   groups point outwards.

537   On the other hand, malonic acid coating (0.4-41.8%) increased the CCN activity of

538   CaCO$_3$ particles regardless of the amount of the coating. The CCN activity of CaCO$_3$

539   particles with malonic acid coating increased with the increase of the amount of the

540   coating. Even a small amount of malonic acid coating (0.4%) significantly enhanced

541   the CCN activity of CaCO$_3$ particles from κ = 0.0028 ± 0.0001 to κ = 0.0123 ±

542   0.0005. Increasing the relative humidity during the coating increased the CCN activity

543   of the CaCO$_3$ particles with malonic acid coating, probably because more CaCO$_3$

544   reacted with malonic acid at a high relative humidity. This process will help to

545   increase the CCN activity.

546   Mineral aerosol is one of the most abundant components of the atmospheric aerosol,

547   but its low water solubility limits its CCN activity. This study showed that

548   water-soluble organic acid coating might significantly enhance the CCN activity of

549   mineral aerosol particles. This could lead to mineral aerosol playing a more important

550   role in cloud formation.

551

552   **Acknowledgments**

553   This study was supported by Forschungszentrum Jülich, the National Natural Science

554   Foundation Committee of China (41421064, 21190051, 41121004), and the China

555   Scholarship Council.

556

557

558 **References**

559 Broekhuizen, K. E., Thornberry, T., Kumar, P. P., and Abbatt, J. P. D.: Formation of cloud
560 condensation nuclei by oxidative processing: Unsaturated fatty acids, J. Geophys.
561 Res.-Atmos., 109, D24206, 10.1029/2004jd005298, 2004.

562 Cakmur, R. V., Miller, R. L., Perlwitz, J., Geogdzhayev, I. V., Ginoux, P., Koch, D., Kohfeld,
563 K. E., Tegen, I., and Zender, C. S.: Constraining the magnitude of the global dust cycle by
564 minimizing the difference between a model and observations, J. Geophys. Res.-Atmos., 111,
565 D06207, 10.1029/2005jd005791, 2006.

566 Charbouillot, T., Gorini, S., Voyard, G., Parazols, M., Brigante, M., Deguillaume, L., Delort,
567 A. M., and Mailhot, G.: Mechanism of carboxylic acid photooxidation in atmospheric
568 aqueous phase: Formation, fate and reactivity, Atmos. Environ., 56, 1-8,
569 10.1016/j.atmosenv.2012.03.079, 2012.

570 Chebbi, A. and P. Carlier (1996). "Carboxylic acids in the troposphere, occurrence, sources,
571 and sinks: A review." Atmospheric Environment 30(24): 4233-4249.

572 Cheng, Y., Li, S. M., Leithead, A., Brickell, P. C., and Leaitch, W. R.: Characterizations of
573 cis-pinonic acid and n-fatty acids on fine aerosols in the Lower Fraser Valley during Pacific
574 2001 Air Quality Study, Atmos. Environ., 38, 5789-5800, 10.1016/j.atmosenv.2004.01.051,
575 2004.

576 Chumpitaz, L. D. A., Coutinho, L. F., and Meirelles, A. J. A.: Surface tension of fatty acids
577 and triglycerides, J. Am. Oil Chem. Soc., 76, 379-382, 10.1007/s11746-999-0245-6, 1999.

578 Cruz, C. N., and Pandis, S. N.: A study of the ability of pure secondary organic aerosol to act
579 as cloud condensation nuclei, Atmos. Environ., 31, 2205-2214,
580 10.1016/s1352-2310(97)00054-x, 1997.

581 DeCarlo, P. F., Kimmel, J. R., Trimborn, A., Northway, M. J., Jayne, J. T., Aiken, A. C.,
582 Gonin, M., Fuhrer, K., Horvath, T., Docherty, K. S., Worsnop, D. R., and Jimenez, J. L.:
583 Field-deployable, high-resolution, time-of-flight aerosol mass spectrometer, Anal. Chem., 78,
584 8281-8289, 10.1021/ac061249n, 2006.

585 Falkovich, A. H., Ganor, E., Levin, Z., Formenti, P., and Rudich, Y.: Chemical and
586 mineralogical analysis of individual mineral dust particles, J. Geophys. Res.-Atmos., 106,
587 18029-18036, 10.1029/2000jd900430, 2001.

588 Falkovich, A. H., Schkolnik, G., Ganor, E., and Rudich, Y.: Adsorption of organic
589 compounds pertinent to urban environments onto mineral dust particles, J. Geophys.
590 Res.-Atmos., 109, D02208, 10.1029/2003jd003919, 2004.

591 Gantt, B., Xu, J., Meskhidze, N., Zhang, Y., Nenes, A., Ghan, S. J., Liu, X., Easter, R., and
592 Zaveri, R.: Global distribution and climate forcing of marine organic aerosol - Part 2: Effects
593 on cloud properties and radiative forcing, Atmos. Chem. Phys., 12, 6555-6563,
594 10.5194/acp-12-6555-2012, 2012.

595

596   Garimella, S., Huang, Y. W., Seewald, J. S., and Cziczo, D. J.: Cloud condensation nucleus
597   activity comparison of dry- and wet-generated mineral dust aerosol: the significance of
598   soluble material, Atmos. Chem. Phys., 14, 6003-6019, 10.5194/acp-14-6003-2014, 2014.

599   Giebl, H., Berner, A., Reischl, G., Puxbaum, H., Kasper-Giebl, A., and Hitzenberger, R.:
600   CCN activation of oxalic and malonic acid test aerosols with the University of Vienna cloud
601   condensation nuclei counter, J. Aerosol Sci., 33, 1623-1634, Pii s0021-8502(02)00115-5,
602   10.1016/s0021-8502(02)00115-5, 2002.

603   Gierlus, K. M., Laskina, O., Abernathy, T. L., and Grassian, V. H.: Laboratory study of the
604   effect of oxalic acid on the cloud condensation nuclei activity of mineral dust aerosol, Atmos.
605   Environ., 46, 125-130, 10.1016/j.atmosenv.2011.10.027, 2012.

606   Hartz, K. E. H., Tischuk, J. E., Chan, M. N., Chan, C. K., Donahue, N. M., and Pandis, S. N.:
607   Cloud condensation nuclei activation of limited solubility organic aerosol, Atmos. Environ.,
608   40, 605-617, 10.1016/j.atmosenv.2005.09.076, 2006.

609   Hatch, C. D., Gierlus, K. M., Schuttlefield, J. D., and Grassian, V. H.: Water adsorption and
610   cloud condensation nuclei activity of calcite and calcite coated with model humic and fulvic
611   acids, Atmos. Environ., 42, 5672-5684, 10.1016/j.atmosenv.2008.03.005, 2008.

612   Haywood, J., and Boucher, O.: Estimates of the direct and indirect radiative forcing due to
613   tropospheric aerosols: A review, Reviews of Geophysics, 38, 513-543,
614   10.1029/1999rg000078, 2000.

615   Herich, H., Tritscher, T., Wiacek, A., Gysel, M., Weingartner, E., Lohmann, U.,
616   Baltensperger, U., and Cziczo, D. J.: Water uptake of clay and desert dust aerosol particles at
617   sub- and supersaturated water vapor conditions, Phys. Chem. Chem. Phys., 11, 7804-7809,
618   10.1039/b901585j, 2009.

619   Ho, K. F., Cao, J. J., Lee, S. C., Kawamura, K., Zhang, R. J., Chow, J. C., and Watson, J. G.:
620   Dicarboxylic acids, ketocarboxylic acids, and dicarbonyls in the urban atmosphere of China,
621   J. Geophys. Res.-Atmos., 112, D22s27, 10.1029/2006jd008011, 2007.

622   Ho, K. F., Lee, S. C., Ho, S. S. H., Kawamura, K., Tachibana, E., Cheng, Y., and Zhu, T.:
623   Dicarboxylic acids, ketocarboxylic acids, alpha-dicarbonyls, fatty acids, and benzoic acid in
624   urban aerosols collected during the 2006 Campaign of Air Quality Research in Beijing
625   (CAREBeijing-2006), J. Geophys. Res.-Atmos., 115, D19312, 10.1029/2009jd013304, 2010.

626   Hori, M., Ohta, S., Murao, N., and Yamagata, S.: Activation capability of water soluble
627   organic substances as CCN, J. Aerosol Sci., 34, 419-448, 10.1016/s0021-8502(02)00190-8,
628   2003.

629   Kawamura, K., and Ikushima, K.: Seasonal-changes in the distribution of dicarboxylic-acids
630   in the urban atmosphere, Environ. Sci. Technol., 27, 2227-2235, 10.1021/es00047a033, 1993.

631   Kawamura, K., Kasukabe, H., and Barrie, L. A.: Source and reaction pathways of
632   dicarboxylic acids, ketoacids and dicarbonyls in arctic aerosols: One year of observations,
633   Atmos. Environ., 30, 1709-1722, 10.1016/1352-2310(95)00395-9, 1996.

634 Kawamura, K., and Bikkina, S.: A review of dicarboxylic acids and related compounds in
635 atmospheric aerosols: Molecular distributions, sources and transformation, Atmospheric
636 Research, 170, 140-160, 10.1016/j.atmosres.2015.11.018, 2016.

637 Keiser, E. H., and Leavitt, S.: On the preparation and the composition of the acid carbonates
638 of calcium and barium, J. Am. Chem. Soc. , 30, 1711-1714, 10.1021/ja01953a008, 1908.

639 Khare, P., et al. (1999). "Atmospheric formic and acetic acids: An overview." Reviews of
640 Geophysics 37(2): 227-248.

641 Koehler, K. A., Kreidenweis, S. M., DeMott, P. J., Petters, M. D., Prenni, A. J., and Carrico,
642 C. M.: Hygroscopicity and cloud droplet activation of mineral dust aerosol, Geophys. Res.
643 Lett., 36, L08805, 10.1029/2009gl037348, 2009.Kumar, P. P., Broekhuizen, K., and Abbatt,
644 J. P. D.: Organic acids as cloud condensation nuclei: Laboratory studies of highly soluble and
645 insoluble species, Atmos. Chem. Phys., 3, 509-520, 2003.

646 Kumar, P. P., Broekhuizen, K., and Abbatt, J. P. D.: Organic acids as cloud condensation
647 nuclei: Laboratory studies of highly soluble and insoluble species, Atmos. Chem. Phys., 3,
648 509-520, 2003.

649 Li, W. J., and Shao, L. Y.: Mixing and water-soluble characteristics of particulate organic
650 compounds in individual urban aerosol particles, J. Geophys. Res.-Atmos., 115, D02301,
651 10.1029/2009jd012575, 2010.

652 Liu, X. H., and Wang, J. A.: How important is organic aerosol hygroscopicity to aerosol
653 indirect forcing?, Environ. Res. Lett., 5, 044010, 10.1088/1748-9326/5/4/044010, 2010.

654 Mkoma, S. L., and Kawamura, K.: Molecular composition of dicarboxylic acids,
655 ketocarboxylic acids, alpha-dicarbonyls and fatty acids in atmospheric aerosols from
656 Tanzania, East Africa during wet and dry seasons, Atmos. Chem. Phys., 13, 2235-2251,
657 10.5194/acp-13-2235-2013, 2013.

658 Moore, R. H., Nenes, A., and Medina, J.: Scanning Mobility CCN Analysis-A Method for
659 Fast Measurements of Size-Resolved CCN Distributions and Activation Kinetics, Aerosol
660 Sci. Technol., 44, 861-871, 10.1080/02786826.2010.498715, 2010.

661 Penner, J. E., Dong, X. Q., and Chen, Y.: Observational evidence of a change in radiative
662 forcing due to the indirect aerosol effect, Nature, 427, 231-234, 10.1038/nature02234, 2004.

663 Petters, M. D., and Kreidenweis, S. M.: A single parameter representation of hygroscopic
664 growth and cloud condensation nucleus activity, Atmos. Chem. Phys., 7, 1961-1971, 2007.

665 Rogge, W. F., Hildemann, L. M., Mazurek, M. A., Cass, G. R., and Simoneit, B. R. T.:
666 Sources of fine organic aerosol .2. Noncatalyst and catalyst-equipped automobiles and
667 heavy-duty diesel trucks, Environ. Sci. Technol., 27, 636-651, 10.1021/es00041a007, 1993.

668 Rogge, W. F., Hildemann, L. M., Mazurek, M. A., Cass, G. R., and Simoneit, B. R. T.:
669 Sources of fine organic aerosol. 9. Pine, oak and synthetic log combustion in residential
670 fireplaces, Environ. Sci. Technol., 32, 13-22, 10.1021/es960930b, 1998.

671

672 Rose, D., Gunthe, S. S., Mikhailov, E., Frank, G. P., Dusek, U., Andreae, M. O., and Poschl,
673 U.: Calibration and measurement uncertainties of a continuous-flow cloud condensation
674 nuclei counter (DMT-CCNC): CCN activation of ammonium sulfate and sodium chloride
675 aerosol particles in theory and experiment, Atmos. Chem. Phys., 8, 1153-1179, 2008.

676 Russell, L. M., Maria, S. F., and Myneni, S. C. B.: Mapping organic coatings on atmospheric
677 particles, Geophys. Res. Lett., 29, 1779, 10.1029/2002gl014874, 2002.

678 Sage, A. M., Weitkamp, E. A., Robinson, A. L., and Donahue, N. M.: Reactivity of oleic acid
679 in organic particles: changes in oxidant uptake and reaction stoichiometry with particle
680 oxidation, Phys. Chem. Chem. Phys., 11, 7951-7962, 10.1039/b904285g, 2009.

681 Schauer, J. J., Kleeman, M. J., Cass, G. R., and Simoneit, B. R. T.: Measurement of emissions
682 from air pollution sources. 1. C-1 through C-29 organic compounds from meat charbroiling,
683 Environ. Sci. Technol., 33, 1566-1577, 10.1021/es980076j, 1999.

684 Sullivan, R. C., Moore, M. J. K., Petters, M. D., Kreidenweis, S. M., Roberts, G. C., and
685 Prather, K. A.: Effect of chemical mixing state on the hygroscopicity and cloud nucleation
686 properties of calcium mineral dust particles, Atmos. Chem. Phys., 9, 3303-3316,
687 10.5194/acp-9-3303-2009, 2009.

688 Sullivan, R. C., Moore, M. J. K., Petters, M. D., Kreidenweis, S. M., Qafoku, O., Laskin, A.,
689 Roberts, G. C., and Prather, K. A.: Impact of Particle Generation Method on the Apparent
690 Hygroscopicity of Insoluble Mineral Particles, Aerosol Sci. Technol., 44, 830-846,
691 10.1080/02786826.2010.497514, 2010.

692 Takegawa, N., Miyakawa, T., Kawamura, K., and Kondo, Y.: Contribution of selected
693 dicarboxylic and omega-oxocarboxylic acids in ambient aerosol to the m/z 44 signal of an
694 aerodyne aerosol mass spectrometer, Aerosol Sci. Technol., 41, 418-437,
695 10.1080/02786820701203215, 2007.

696 Tang, M. J., Whitehead, J., Davidson, N. M., Pope, F. D., Alfarra, M. R., McFiggans, G., and
697 Kalberer, M.: Cloud condensation nucleation activities of calcium carbonate and its
698 atmospheric ageing products, Phys. Chem. Chem. Phys., 17, 32194-32203,
699 10.1039/c5cp03795f, 2015.

700 Yamashita, K., Murakami, M., Hashimoto, A., and Tajiri, T.: CCN Ability of Asian Mineral
701 Dust Particles and Their Effects on Cloud Droplet Formation, Journal of the Meteorological
702 Society of Japan, 89, 581-587, 10.2151/jmsj.2011-512, 2011.

703 Zhao, D. F., Buchholz, A., Mentel, T. F., Muller, K. P., Borchardt, J., Kiendler-Scharr, A.,
704 Spindler, C., Tillmann, R., Trimborn, A., Zhu, T., and Wahner, A.: Novel method of
705 generation of Ca(HCO(3))(2) and CaCO(3) aerosols and first determination of hygroscopic
706 and cloud condensation nuclei activation properties, Atmos. Chem. Phys., 10, 8601-8616,
707 10.5194/acp-10-8601-2010, 2010.

Table 1. Mode diameters, chemical compositions, and κ values of CaCO$_3$ aerosol particles (size selected by DMA at 101.8 nm) before (uncoated) and after coating with oleic (OA) or malonic acid (MA) at 30–80 °C.

	Mode diam. [nm]	OA per particle (marker $m/z41$) [10^{-12} µg]	MA per particle (marker $m/z42$) [10^{-12} µg]	Organic volume fraction [%]	κ
Uncoated					
CaCO$_3$ 30-80 °C	101.8	(backgr.: 2.4±0.79)	(backgr.: 1.4±0.42)	0.0	0.0028±0.0001
Oleic acid					
CaCO$_3$+Oleic acid 30 °C	101.8	3.3±1.7		0.7	
CaCO$_3$+Oleic acid 40 °C	101.8	6.3±2.6		1.3	
CaCO$_3$+Oleic acid 50 °C	101.8	13±3.3		2.5	
CaCO$_3$+Oleic acid 60 °C	105.5	21±1.1		4.1	
CaCO$_3$+Oleic acid 70 °C	109.4	86±3.3		14.8	0.0237±0.0006
CaCO$_3$+Oleic acid 80 °C	121.9	350±12		41.8	0.0673±0.0016
Malonic acid					
CaCO$_3$+Malonic acid 30 °C	101.8		3.5±0.30	0.4	0.0123±0.0005
CaCO$_3$+Malonic acid 40 °C	101.8		7.1±1.2	0.8	0.0231±0.0008
CaCO$_3$+Malonic acid 50 °C	101.8		14±1.9	1.6	0.0380±0.0012
CaCO$_3$+Malonic acid 60 °C	101.8		40±1.7	4.5	0.1056±0.0023
CaCO$_3$+Malonic acid 70 °C	109.4		170±8.5	15.5	0.1813±0.0031
CaCO$_3$+Malonic acid 80 °C	121.9		640±26	41.8	0.3001±0.0062
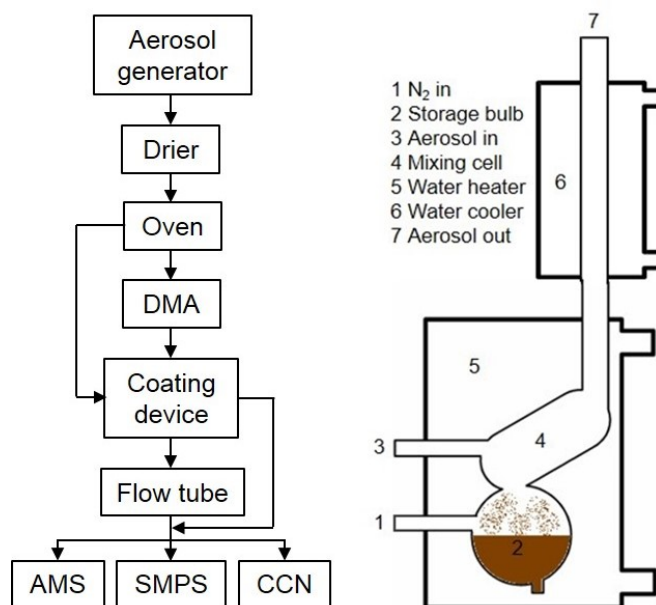
Figure 1. Schematics of the experimental set up (left side). $CaCO_3$ aerosol is generated by spray-drying of saturated $Ca(HCO_3)_2$ solutions and tempering the aerosol passing through an oven at 300°C. The *poly-disperse* $CaCO_3$ aerosol is either led directly to the coating device (right side, after Roselli, 2006) or led to a differential mobility Analyzer (DMA) for size selection first. Optional, a flow tube can be switched into the pass to enhance the reaction time of the coated particles. The stream of coated particles is finally split to the analytical instruments, namely aerosol mass spectrometer (AMS), scanning mobility particle sizer (SMPS) and CCN counter.
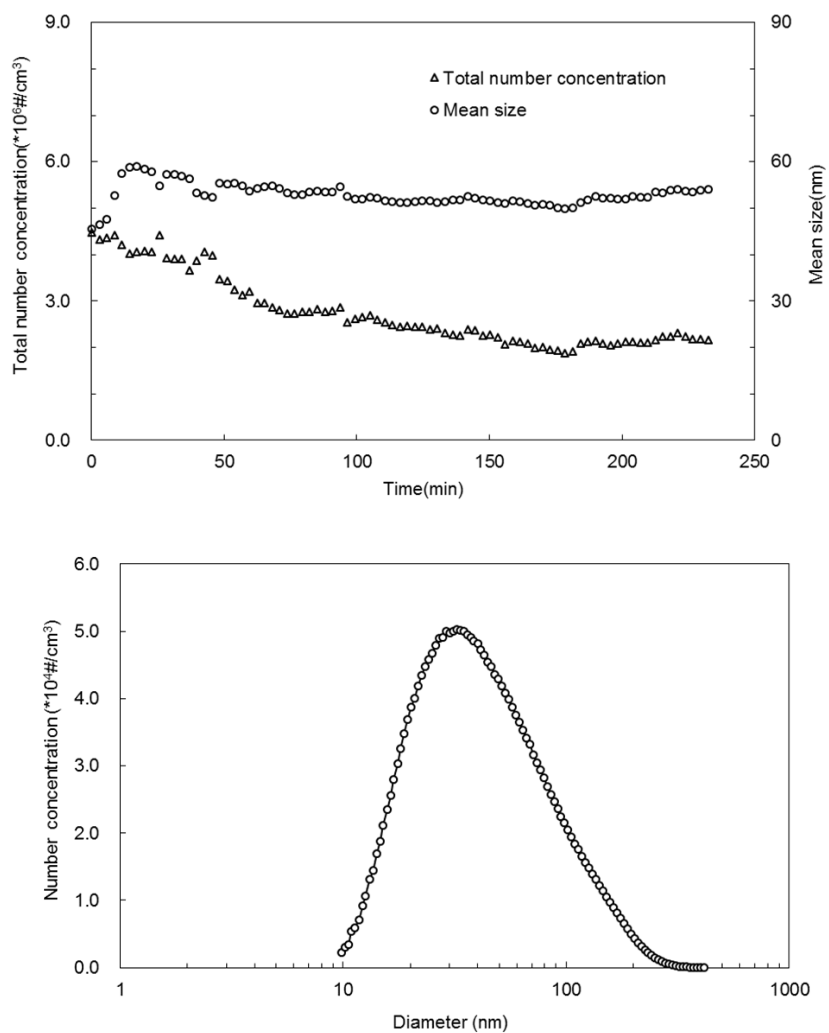
Figure 2. Total number concentration and mean diameter of $CaCO_3$ aerosol particles generated as a function of the spraying time (upper panel). Typical size distribution of the $CaCO_3$ aerosol after 70 min spraying (lower panel).
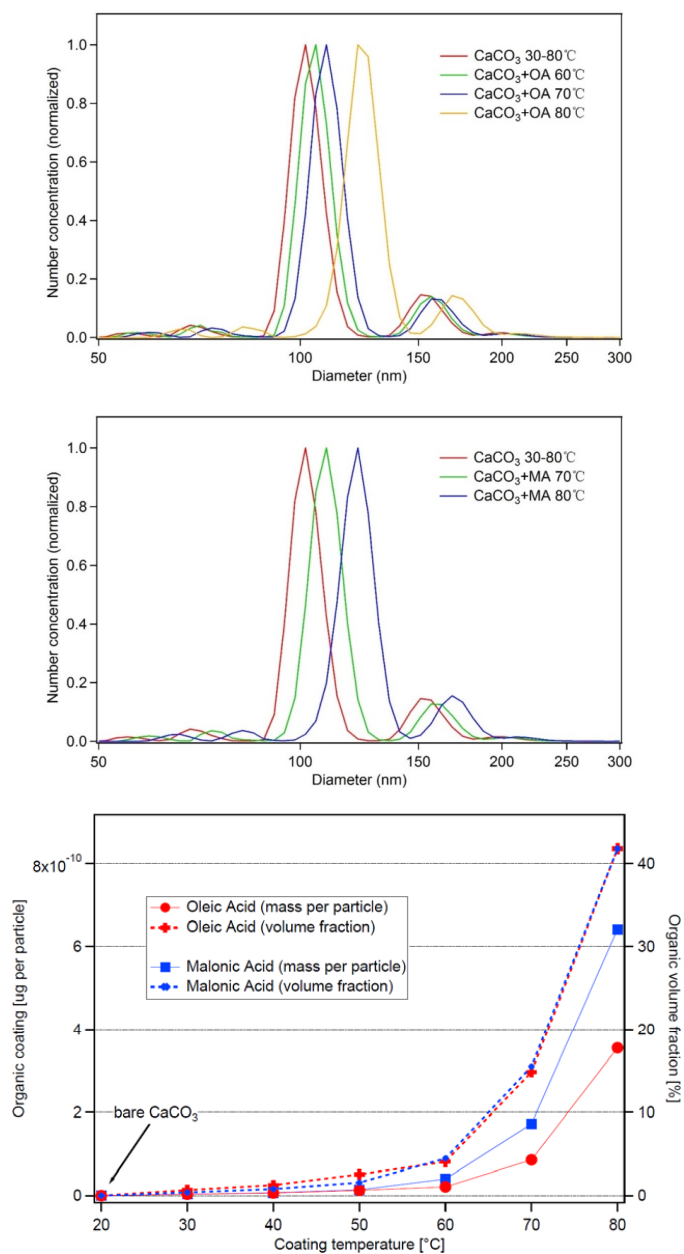
Figure 3. Size distribution of monodisperse CaCO$_3$ aerosol particles with mode diameter 101.8 nm of the CaCO$_3$ core before and after coating with oleic acid (top panel) or malonic acid (middle panel). Coating amount and organic volume fraction for oleic and malonic acid as a function of the coating temperature for the same experiments (bottom panel, compare Table 1).
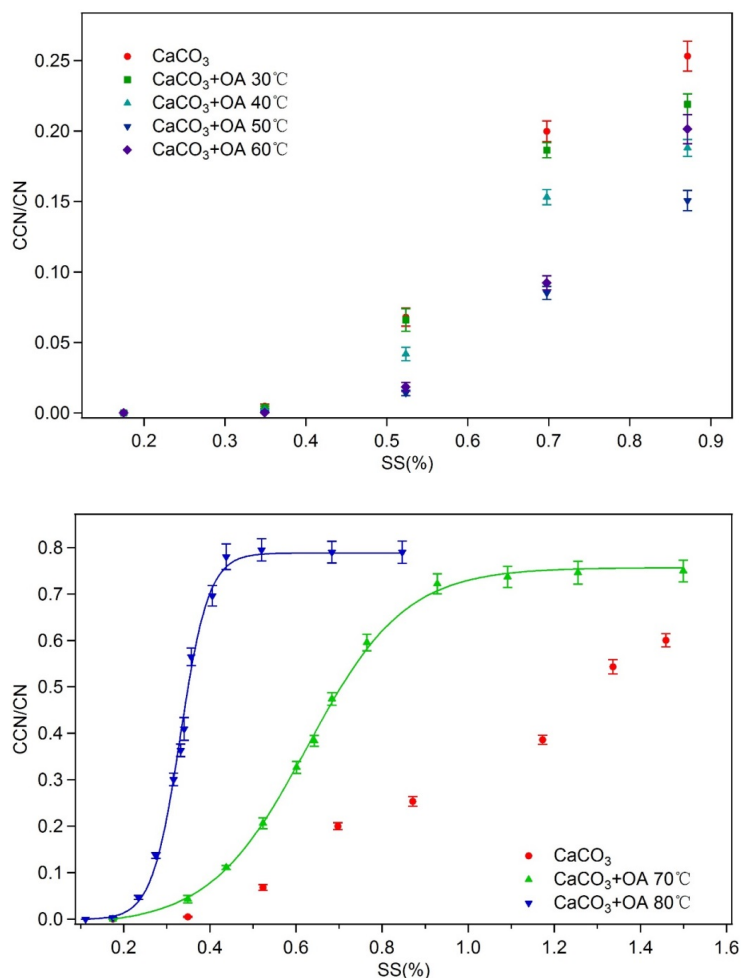
Figure 4. Activated fractions (CCN/CN) of *monodisperse* CaCO$_3$ aerosol particles (size selected at 101.8 nm) at different supersaturations before and after oleic acid coating. With increasing coating temperatures of 30-50 ℃ the activated fraction decreases. At 60°C this trend turns. Considering the invariant mode diameter at 30-50 ℃, the increased mode diameter at 60 ℃, and the reduced activated fraction simultaneously, the CCN activity of the coated CaCO$_3$ particles at 30-60 ℃ was lower than that of the uncoated CaCO$_3$ particles (top panel). At coating temperatures of 70-80 ℃ the activated fractions, thus CCN activities, are higher than for bare CaCO$_3$ and increase with coating temperature. In these two cases all particles are activated at the highest SS and SS$_{crit}$ and κ can be determined from the turning point of the Gaussian fit (bottom panel, compare Table 1).
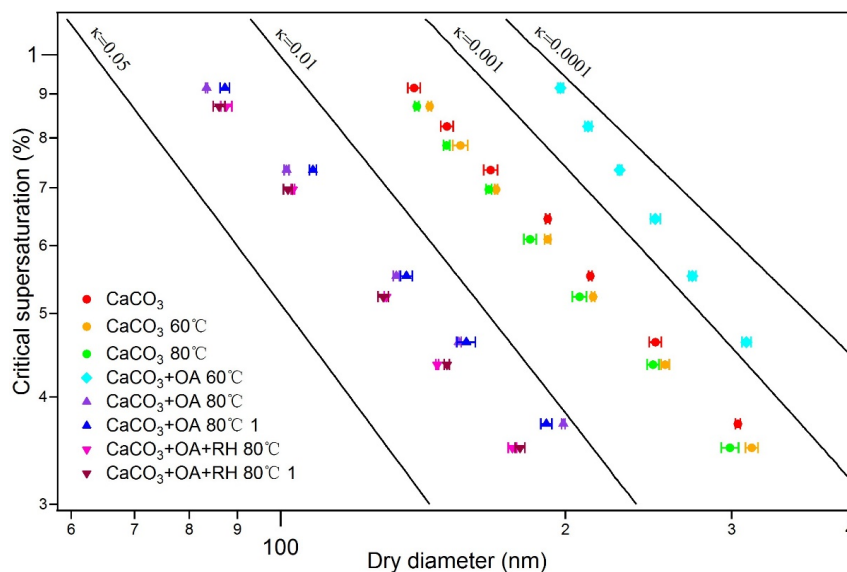
Figure 5. Critical dry diameters at different super-saturations (SS) of *poly-disperse* $CaCO_3$ aerosol before (circles) and after oleic acid coating. Experiments were performed at 60°C (turquoise diamond) and 80°C (triangles) coating temperatures. The flow tube experiments at 80° C were performed (indicated by the 1) at dry (normal) case (blue tringles) and at 47% RH (brown triangles). The effect of the coating temperature on the $CaCO_3$ core is negligible (red, green, and orange circles). As for the monodisperse case in Figure 4, at 60° coating temperature the particles are less CCN active than bare $CaCO_3$ while at 80°C the coated particle more CCN active. The presence of water in the coating process enhances CCN activity. The increasing of residence time (23.7 s) of the coated aerosol in the flow tube had no significant effect on CCN activity in both experiments.
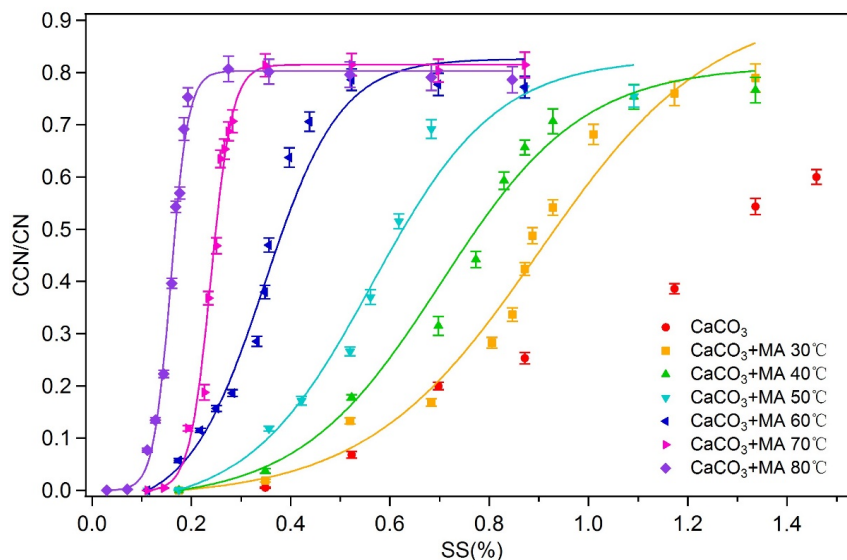
Figure 6. Activated fractions (CCN/CN) of *monodisperse* CaCO₃ aerosol particles (size selected at 101.8 nm) at different supersaturations before and after malonic acid coating. With increasing coating temperatures of 30-80 ℃ the activated fraction, thus CCN activity, increase compared to bare CaCO₃ particles. All coated particles can be activated at sufficiently high SS and SS_crit and κ can be determined (compare Table 1).
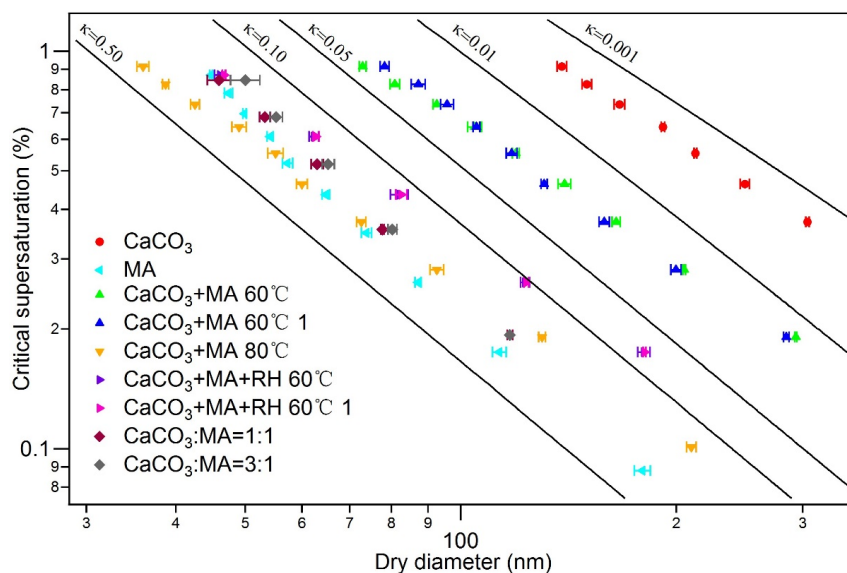
Figure 7. Critical dry diameters at different super-saturations (SS) of *poly-disperse* $CaCO_3$ aerosol before (circles) and after malonic acid coating (triangles). Experiments were performed at 60°C and 80°C coating temperatures. The results are similar to the monodisperse case in Figure 6. Critical dry diameters as a function of SS are also shown for malonic acid particles and particles that were generated by spraying mixed solution with molar ratios of $CaCO_3$/malonic acid of 1:1 and 3:1. The CCN activity decreases with increasing $CaCO_3$ content. The flow tube experiments at 60 °C were performed (indicated by the 1) at dry (normal) condition (blue tringles) and at 47% RH (magenta triangles). The presence of water in the coating process enhances CCN activity. The increasing of residence time (23.7 s) of the coated aerosol in the flow tube had no significant effect on CCN activity in both experiments.